FACTA UNIVERSITATIS (NIŠ)
SER.: ELEC. ENERG. vol. 18, no. 3, December 2005, 395-419

Toward Simple Robust Control of Single or Current-Sharing DC/DC Converters Driven by Deterministic or Random Switching

Dedicated to Prof. M. Stojić on the occasion of his 65th birthday

Aleksandar Ž. Rakić and Trajko B. Petrović

Abstract: In this paper, the multivariable robust approach is used to obtain simple controllers for both single and current- sharing (paralleled) DC/DC converters. Linear time-invariant nominal model of the power stage is derived and asymptotic uncertainty bounds are constructed to cover the parametric uncertainty, nonlinear effects in control, CMC switching effects and random switching control. Robust model of the current-sharing converters is developed and joint framework for the frequency domain robust design is proposed for both single and current-sharing configurations. The feasibility of the approach is demonstrated by two design examples: random control of the single unit buck converter and deterministic control of the three paralleled buck units. Several robust controllers are designed and verified for robustness and performance in the closed-loop with the Matlab and pSpice models.

Keywords: DC/DC converter, current sharing, pulse width modulation, random switching, robust modeling, robust control, simple controllers.

1 Introduction

DC/DC converters [1, 2] are standard components in computer and telecom power supply systems. High power demands, modularity and redundancy reasons bring out the need of several converter units sharing the current to be supplied to the system. From the control point of view, converters in current sharing parallel arrangement make a multivariable plant to be controlled. Classical small-signal analysis

Manuscript received August 29, 2005.

The authors are with Faculty of Electrical Engineering, University of Belgrade, Bulevar kralja Aleksandra 73, 11120 Belgrade, Serbia and Montenegro (e-mails: [rakic, petrovic]@etf.bg.ac.yu

and control design in the frequency domain are discussed in [3]-[10]. Advanced nonlinear techniques in control are presented in [11, 12].

The robustness of the control is always the main point and major problem due to fact that a model of a power supply is always an approximation of the real system. Furthermore, the dynamics of a power system may change during long-term operation, mainly because of the power components' variations. To address the difference between modeled and true systems, various measures of robustness are used [13]-[16]. The single DC/DC converter robust analysis and control synthesis are conducted in [17]-[20]. Robust modeling and control design of random switching converters are discussed in [21, 22]. The multivariable H_∞ linear robust analysis of the parallel operating converter units is the subject of the papers [23, 24]. The analysis of the control system itself is discussed in [25]. Robust design for parallel operating DC/DC converters is presented in papers [26]-[28]. The main drawback of the linear robust approach is the high order of the fully multivariable controllers, often unacceptable for the application both in analog and digital control.

The purpose of this paper is to investigate the possibility to use robust linear theory to obtain simple controllers for both single and current-sharing DC/DC converters, applicable according to industrial needs along with deterministic (PWM) and random control. The analysis of the proposed control design will be conducted within *Matlab and Signal Processing Toolbox, The MathWorks Inc, MA-USA*. and *pSpice, Cadence Design Systems Inc, CA-USA*. The paper is organized in sections. Sect. 2 describes the robust modeling of the power stage. Sect. 3 considers the modeling of the current-sharing (paralleled) configuration of converters. Sect. 4 is the place where the framework for robust control of the converters is discussed. The development and verification of the closed-loop design on nonlinear models of single buck random controlled and three parallel conventionally (PWM) controlled buck DC/DC converters is the subject of Sect. 5. The conclusion is presented in Sect. 6.

2 Power-Stage Modeling

2.1 Nominal model

DC/DC converter consists of nonlinear subsystem, dedicated to fast switching of unregulated DC input voltage, and linear subsystem for filtering of obtained switched voltage signal. Fig. 1 represents buck and boost DC/DC converters that will be considered for analysis and modeling in this section.

Input unregulated voltage is denoted with v_{IN}, R is the nominal resistive load of converter, L and R_L represent inductivity and its parasitic series resistance, C and R_C are capacity and its parasitic series resistance. Nonlinear subsystem for switching

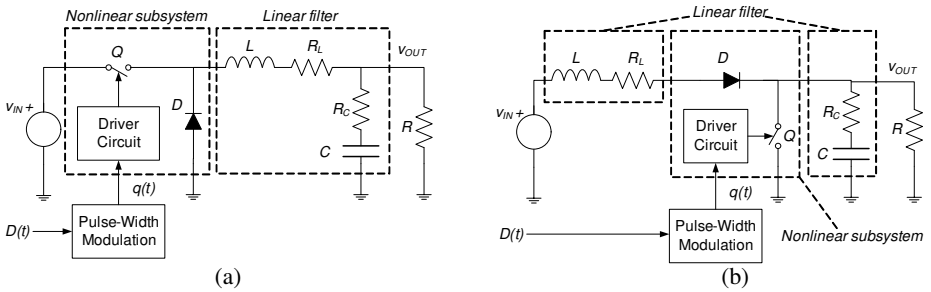

Fig. 1. Power stage a DC/DC converter: (a) Buck topology, (b) Boost topology.

consists of diode D and switching element Q, which is usually energetic BJT or MOSFET. Transistor control is done through the driver circuit, according to control signal $q(t)$, which has discrete values of 0 or 1 (switch on and switch off). $q(t)$ is assembly of rectangular nonoverlapping impulses, result of some modulation technique over continual control variable of switching $D(t) \in (0,1)$. Modulated control $q(t)$ directly influences DC value and frequency response of current and voltage of DC/DC converter.

Fig. 2 represents typical shape of signal $q(t)$, with characteristic variables of i-th period of switching: ε_i - time from the beginning of i-th switching cycle to the moment of transistor turn-on, D_i - duty ratio (relative transistor turn-on time on cycle- length basis), T_i - period of i-th cycle and ξ_i - start time of i-th cycle.

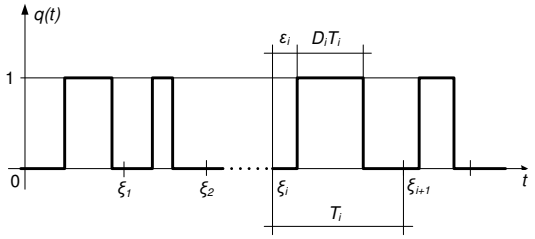

Fig. 2. Typical shape of control variable signal $q(t)$.

Taking nonlinear element as ideal, equivalent circuit of converter, that uses $q(t)$ to model nonlinearity effect of the switching, can be developed (Fig. 3).

In the case of deterministic PWM switching, there is no gap between the start of the cycle and the moment of transistor turn-on ($\varepsilon_i \equiv 0$). Also, cycle periods are constant ($T_i \equiv T$). Higher frequency content is neglected in nominal modeling and only mean value of signal in the switching period is considered: $\overline{q}(t \in (t_i, t_{i+1})) = D_i$. As the switching period is significantly smaller than the time-constants of the linear part of the circuit, discrete array D_i describes in full the properties of the continuous

control signal $D(t)$ in the bandwidth. $D(t)$ replaces $q(t)$ in the equivalent circuit in Fig. 3. By the averaging in the switching period, nonlinearity of PWM switching is eliminated from further nominal modeling.

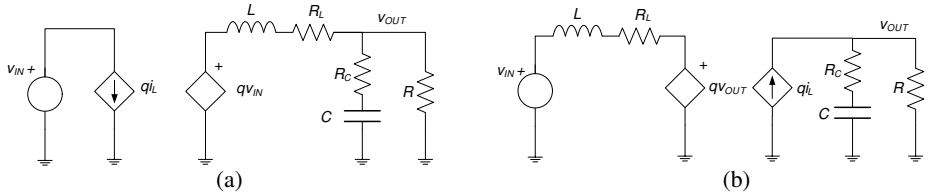

Fig. 3. Equivalent circuit of converter: (a) Buck topology, (b) Boost topology.

Model of the converter for the small signal is obtained from the equivalent circuit by means of linearization of the state- variables' (output voltage v_{OUT} and inductor current i_L) dependencies on the control variable D and disturbance variables (input voltage deviation v_{IN} and load current deviation i_G).

In summary, state-space averaging is characterized by following approach and results:

- operating-point (DC values of output voltage V_{OUT} and inductor current I_L) is obtained, depending on nominal values of control D_0 , input voltage supply V_{IN} and parameters of the linear part of the circuit $\Lambda = \{R, L, C, R_L, R_C\}$;
- Laplace-transform of v_{OUT} and i_L linearized dependencies on small changes of control $(d = D - D_0)$, input voltage $(v_{in} = v_{IN} - V_{IN})$ and load current $(i_g = i_G - I_G)$ represent transfer functions in the small-signal model:
  1) transfer from control to output voltage: $Pv_(s) = v_{out}(s)/d(s)$, $i_g = v_{in} = 0$;
  2) transfer from control to inductor current: $P_i(s) = i_L(s)/d(s)$, $i_g = v_{in} = 0$;
  3) audio susceptibility: $A_S(s) = v_{out}(s)/vin(s)$, $i_g = d = 0$;
  4) output impedance: $Z_{out}(s) = v_{out}(s)/i_g(s)$, $v_{in} = d = 0$;
  5) transfer from the load to inductor current: $T_c(s) = i_L(s)/i_g(s)$, $v_{in} = d = 0$;
  6) input admittance: $Y_{in}(s) = i_L(s)/v_{in}(s)$, $ig = d = 0$.

In Fig. 4 linear small signal model of DC/DC converter power stage is presented along with disturbance sources v_{in} and i_g and transfer functions from them to the state variables.

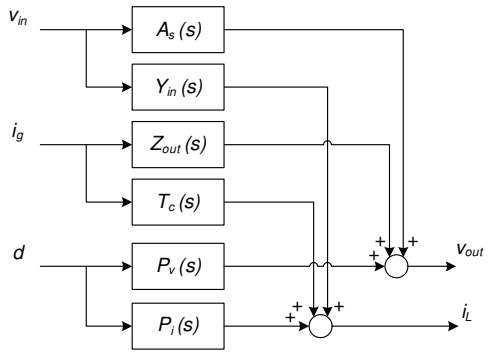

Fig. 4. Linear model of DC/DC converter power stage.

For nominal converter modeling, as the primary task of control is the voltage setpoint tracking and disturbance rejection, functions of interest are $P_v(s)$ and $P_i(s)$, as the transfer functions from the control to the state-variables. Those transfer functions for buck and boost converters are given in Table 1. Background on state-space averaging and presented nominal model transfer functions can be found in [1, 2].

Table 1. Buck and Boost DC/DC converter linear model transfer function.

BUCK	$P_v(s) = \dfrac{V_{IN}R(R_cCs+1)}{LC(R+R_C)s^2+[(RR_L+RR_C+R_LR_C)C+L]s+R+R_L}$
	$P_i(s) = \dfrac{V_{IN}[(R+R_C)Cs+1)}{LC(R+R_C)s^2+[(RR_L+RR_C+R_LR_C)C+L]s+R+R_L}$
BOOST	$P_v(s) = k\dfrac{(R_CCs+1)[R^2(1-D_0)^2-RR_L-R_LR_C-(R_L+R_C)Ls]}{a_2s^2+a_1s+a_0}$
	$P_i(s) = k\dfrac{2R(1-D_0)+R_C-[R^2C(1-D_0)+RR_CC(D_0-2)-R_C^2Cs]}{a_2s^2+a_1s+a_0}$
	$k = \dfrac{(R+R_C)RV_{IN}}{RR_L+RR_C(1-D_0)+R_LR_C+R^2(1-D_0)^2}$, $a_2 = (R+R_C)^2LC$, $a_1 = (R+R_C)L+RR_C(R+R_C)(1-D_0)C+R_C^2R_LC+2RR_LR_CC+R^2R_LC$, $a_0 = RR_L+RR_C(1-D_0)+R_LR_C+R^2(1-D_0)^2$.

2.2 Uncerainty and Robustness

Linear model is not able to describe the behavior of the inherently nonlinear plant. Models of the finite order always introduce uncertainty in modeling. The idea of the robust control is referring control synthesis, its performance and stability, not

only to the *nominal plant model*, but also to the whole family of models in the area of permitted uncertainty of the modeling (perturbations are bounded). So, as new terms appear *robust performance* - guarantied performance of the control system for all systems in the uncertainty region, and *robust stability* - stability of all possible systems inside the uncertainty modeling bounds.

In the robustness analysis of the control systems three standard models of unstructured uncertainty are used: additive uncertainty:

$$\tilde{P} = P + l_A(s)\Delta_A \tag{1}$$

multiplicative input uncertainty:

$$\tilde{P} = P(1 + l_{MI}(s)\Delta_{MI}) \tag{2}$$

multiplicative output uncertainty:

$$\tilde{P} = (1 + l_{MO}(s)\Delta_{MO})P \tag{3}$$

where $\tilde{P}$ is the real plant, P - its model used in the control synthesis, $l_A(s)$, $l_{MI}(s)$ and $l_{MO}(s)$ - bounds of allowed uncertainty of the robust modeling, and Δ_A, Δ_{MI} and Δ_{MO} represent unknown, but unity normed values of the unstructured uncertainty of modeling.

In the context of the robust modeling of DC/DC converter, the most convenient uncertainty representation is the multiplicative input uncertainty (2), because the modeling uncertainty is effectively added to uncertainty of modeling in the plant input, as the uncertainty of the control system, which is really the case when the modulation is used in control. Furthermore, this choice of uncertainty representation enables the use of the robust theory in random modulation in control, which is effectively also the uncertainty in the control system i.e. on the plant input. Multiplicative input uncertainty is represented in Fig. 5, where $l_{MI}(s)$ is the uncertainty bound and Δ_{MI} - unknown normalized ($\|\Delta_{MI}\| < 1$) perturbation corresponding to the unstructured uncertainty of the modeling.

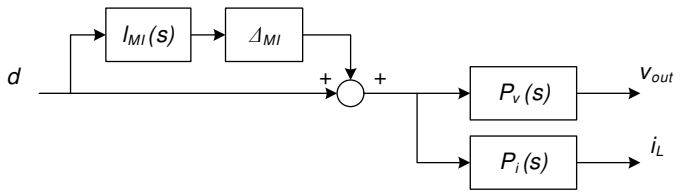

Fig. 5. Robust modeling uncertainty representation.

Bound of the multiplicative input uncertainty is developed to asymptotically describe the uncertainty: on low frequencies it has the value of the maximal error

of the transfer function P_v DC gain estimation, after the transmission zero rises with the slope of 20 dB per decade, reaches 0 dB level before the half of the switching frequency and remains on the constant level after the pole in high frequencies, to preserve causality of the transfer function $l_{MI}(s)$.

Transmission zero, on one hand, is to be selected low enough in frequencies to start raising of uncertainty bound to cover neglected dynamics of the converter in high frequencies. On the other hand, even at the stage of modeling, one should have in mind that the inverse function $1/l_{MI}(s)$ represents the worst-case complementary sensitivity function $T_{WC}(s)$ of the robust control design, so the choice of the zero position in the transfer function $l_{MI}(s)$, as a pole of $T_{WC}(s)$, directly limits the bandwidth of the H_∞/μ -optimal control designed later on. Typically, this choice is the subject of compromise between the antagonistic demands to be solved separately for each design case. Once the zero is selected, pole is placed on at least 4 - 10 times higher frequency to provide $T_{WC}(s)$ roll-off to values low enough in high frequencies, enabling good disturbance rejection of high frequency noise and robustness to unmodeled dynamics.

2.3 Uncertainty Modeling Covering the Nonlinearity of the Converters

All the transfer functions, in the general nonlinear case, are functions of linear circuit elements Λ, but also functions of converter operating point i.e. stationary control value $D = D_0$. Nominal model of the converter is, therefore, changing if the excursions of the control variable are considerable, which is the case in the disturbance rejection actions.

Robust modeling can cover also the effects of the plant model perturbations caused by the nonlinearity i.e. change of the operation point due to the disturbance rejection actions. Namely, one can assume plant model to be changing in some bounds of the modeling uncertainty, although one knows the uncertainty is not due to the parameter tolerances, but due to the change of the linear model of the converter, as the function of the operating point change. Uncertainty bound is to be chosen to have DC gain greater than maximal change of the DC gain in the whole family of the transfer functions (in the range of all possible controls $D \in (D_{min}, D_{max})$) comparing to DC gain of the nominal transfer function (determined by the nominal control D_0). Dynamics of the uncertainty bound transfer function is designed in the same way as for the uncertainty coverage of the parameter tolerances in the previous section.

The problem arising in control design is the plant models often change drastically i.e. perturbations are, even for DC gain, close to 100 % or even greater. Robust control theory cannot solve that kind of uncertainty problems: optimal controllers cannot be found or they are too conservative to be applied. But, the solution lies

in the proper choice of the nominal model. When the model linearized around the real operating point of the converter is not able to provide acceptable uncertainty bounds, then different nominal model is to be chosen. The appropriate model is the one minimizing uncertainty bounds in the bandwidth for the whole family of possible plants.

Although control afterward is not to be designed for the plant linearized around the real operating point, this can be done due to fact the robust stability and robust performance are to be satisfied in the robust control design for the whole family of possible plants and therefore also for the "real" nominal model i.e. the one linearized around the real operating point.

2.4 Uncertainty Modeling of Current Mode Controlled (CMC) Converters

All presented discussion to this point referred the converter modeling in so called voltage mode control (VMC) i.e. when the control is applied only on the basis of sensing the output voltage of the converter. Switching effects appear as the special phenomena of the current mode control i.e. when control is based on sensing both the output voltage and the output current of the converter. In the well known paper [3] appropriate model is developed for CMC converters. CMC converter model is only the extension of the model given in Fig. 4, because the transfer functions of the nominal CMC converter model are the same as ones developed for the VMC converter model. Only current feedback loop is to be modeled adequately. CMC modeling setup is depicted in Fig. 6.

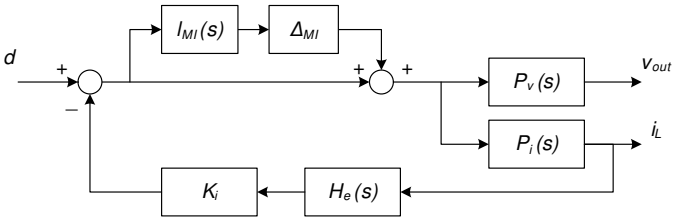

Fig. 6. CMC modeling setup.

Block K_i is the current feedback linear gain and $H_e(s)$ is modeling the sampling effect in CMC. Block $H_e(s)$ is found to be [3]:

$$H_e(s) = \frac{sT_s}{e^{sT_s} - 1}, \tag{4}$$

or, as very good approximation, up to the half of the switching frequency:

$$H_e = 1 + \frac{s}{\omega Q_z} + \frac{s^2}{\omega_n^2}, \quad Q_z = -\frac{\pi}{T_s}, \quad \omega_n = \frac{\pi}{T_s}, \tag{5}$$

where T_s is the sampling period.

Fig. 7 gives the frequency plot of $H_e(s)$ up to the half of the switching frequency. In the bandwidth of the regulation its contribution is surely less than 4dB.

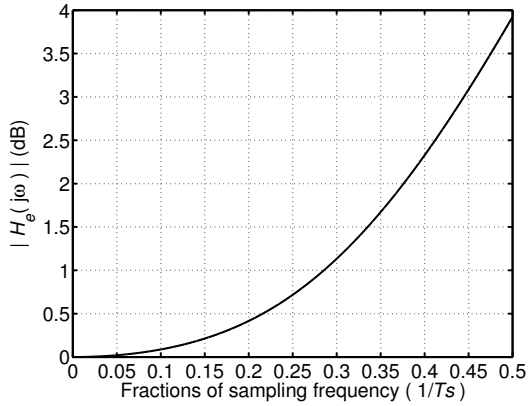

Fig. 7. Frequency plot of $H_e(s)$.

So, reasonable proposition of the modeling of the switching effect in the current loop is to join this effect to general uncertainty of modeling, neglect the block $H_e(s)$ in the control setup and use the same model as for the voltage mode control but with the current loop closed by just the linear gain K_i.

2.5 Random Switching as Uncertainty in Modeling

In the process of random modulation, the switching control variable $D(t) = E(q(t))$ can be generated in several ways, randomly varying one of three variables of the modulated control $q(t)$ pulse shape $u_i(t - \varepsilon_i)$ (depicted in Fig. 2): D_i - duty ratio for the i-th cycle of the switching, ε_i - position of the start of the impulse in the i-th cycle, and the period of the switching T_i.

Random change of variables ε_i, D_i or T_i shapes the frequency spectrum of the output voltage i.e. reduces the discrete component (harmonic) on the frequency of commutations.

Randomness of ε_i and D_i do not affect the periodicity of the sequence of the modulated control signal $q(t)$, so Random Pulse Position Modulation (RPPM) and Random Pulse Width Modulation (RPWM) are periodic modulations, while techniques which include varying of the period of switching are called aperiodic modulations: DFIX - when D_i is kept to deterministic control value $D(t)$, and AFIX - when on-time of the switch $A = DT$ is kept deterministic. Spectral formulas for

mentioned random modulation, derived in [21], are:

$$S_q^{RPWM}(\omega) = \frac{|U_0(\omega)|^2}{T}(1-|P_\varepsilon(\omega)|^2) + \frac{|U_0(\omega)|^2|P_\varepsilon(\omega)|^2}{T^2}\sum_{k-\infty}^{+\infty}\delta(\omega - k\frac{2\pi}{T}), \quad (6)$$

$$\begin{aligned} S_q^{RPWM}\omega = &\frac{1}{\omega^2 T}[2(1-\Re\{P_D(T\omega)\}) - |1-P_D(T\omega)|^2] \\ &+ \frac{1}{\omega^2 T^2}|1-P_D(T\omega)|^2\sum_{k=-\infty}^{+\infty}\delta(\omega - k\frac{2\pi}{T}) \end{aligned} \quad (7)$$

$$S_q^{DFIX}(\omega) = \frac{2}{\omega^2 T}[1-\Re\{P_T(D\omega)\} + \Re\{\frac{(1-P_T(D\omega))(P_T((1-D)\omega))}{1-P_T(\omega)}\}] \quad (8)$$

$$S_q^{AFIX}(\omega) = \frac{|U_0(\omega)|^2}{T}[1+2\Re\{\frac{P_T(\omega)}{1-P_T(\omega)}\}] \quad (9)$$

where $U_0(\omega)$ is the Fourier transform of rectangular pulse with unity intensity (amplitude), width $D_i T_i$, and start in time zero, $P_\varepsilon(\omega)$, $P_D(\omega)$ and $P_T(\omega)$ are the Fourier transforms of the applied probability density function (pdf) of random variables ε, D or T, consequently.

In the context of the robust modeling of the random switching DC/DC converter, the most convenient uncertainty representation is the multiplicative input uncertainty, because neglected continuous modulation noise is effectively added to uncertainty of modeling in the plant input, i.e. uncertainty of the control system, which really is the case with the random modulation. Uncertainty due to random control is represented by its bound $l_{RMI}(s)$ and Δ_{RMI} - unknown but unity normed perturbation of random modeling, containing continuous noise spectrum of the control q.

Random switching effect in control are to be added to the deterministic uncertainty in modeling of the converter, which is not related to the nature of control, but with component tolerances of the converter itself. No correlation in these effects enables simple addition of the modeling uncertainty due to random effects in control to the parametric uncertainty of the deterministic switching converter modeling.

Using the same guidelines as for the deterministic modeling, random switching multiplicative input uncertainty bound $l_{RMI}(s)$, on low frequencies, has the value of the maximal excursion of the control variable from its steady state $R = \max(D(t) - D_0)$ in the process of random switching control. As this value is assumed to be significantly greater than the frequency peak of the continuous noise spectrum in the bandwidth of the control, random switching effect in control can be included in the uncertainty description just by adequate increase of the deterministic switching uncertainty bound $l_{DET}(s)$ DC gain in amount given to the randomization effects.

Therefore, random effects can be included into the uncertainty bound $l_{MI}(s)$ of converter modeling in two ways:

1. keeping the deterministic uncertainty bound $l_{MI}(s) = l_{DET}(s)$, and concerning one part of the modeling uncertainty covers parametric uncertainty, while the other one covers the random effects, which effectively narrows permitted tolerance of the linear circuit elements;
2. adding R, as a net effect of random uncertainty modeling on low frequencies, to the deterministic bound DC gain $l_{MI}(s=0) = l_{DET}(s=0) + R$ and keeping the dynamics that describes asymptotic behavior of the modeling uncertainty in deterministic case.

It this way, two conditions will be fulfilled:

1. uncertainty bound of random switching converter will cover deterioration of experimental spectrum from theoretically anticipated, enabling controller synthesis for existing parametric uncertainty level of deterministic switching converter with random control uncertainty added,
2. uncertainty bound of deterministic switching modeling will cover in full the effects of random control, enabling use of existing controllers for deterministic switching converters, with remark that allowed parametric uncertainty of modeling effectively dropped for the value given to the random uncertainty covering.

3 Robust Modeling of the Current-Sharing (Paralleled) Converters

The simplified block diagram of n paralleled units and control loops is presented in Fig. 8. Each unit j has PWM driver, which applies duty-ratio d_j from the control subsystem to power stage switch or switches. Outer voltage-control loop is managed by the joint voltage controller $K_v(s)$, trying to achieve voltage reference v_{ref} at the voltage output v_{out} of the paralleled converters i.e. at the input of the load. Each converter j provides measurement of its current i_j, which is driven by the current controller $K_{ij}(s)$ to attain reference current i_{ref}. Choice of weights α_j determines the paralleling scheme: democratic current sharing is established if all of α_j are equal to $1/n$, while master-slave current sharing is obtain with $\alpha_1 = 1$, $\alpha_2 = \alpha_3 = \ldots = \alpha_n = 0$, and $K_{i1}(s) = 0$.

In the paper [23] multivariable model of the parallel operating converters is obtained as:

$$v_{out}(s) = \frac{1}{\frac{1}{R} + \sum_{i=1}^{n} \frac{1}{Z_{outi}(s)}} \sum_{i=1}^{n} \frac{P_{vi}(s)}{Z_{outi}(s)} d_i(s) = \sum_{i=1}^{n} P'_{vi}(s) d_i(s) \tag{10}$$

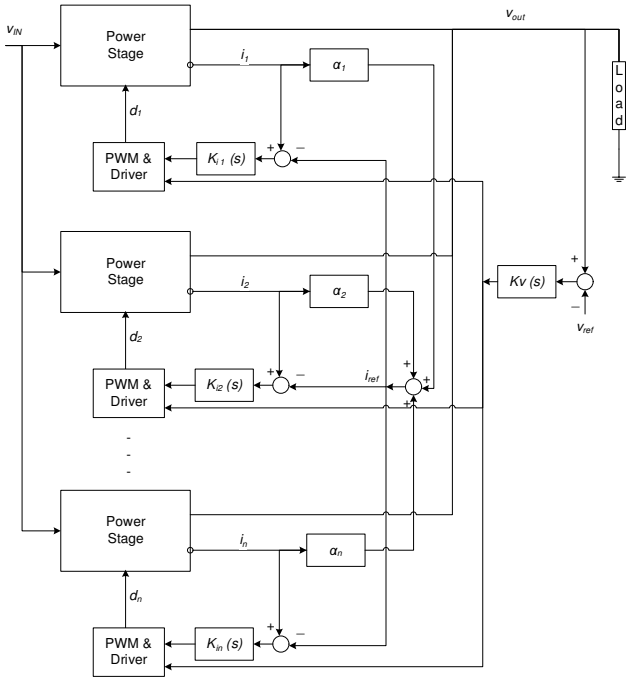

Fig. 8. Block diagram of n paralleled DC/DC converters with current sharing loops.

$$i_{Li}(s) = P_{ii}(s)d_i(s) \qquad i = 1,2,\ldots,n, \tag{11}$$

where R is the nominal load, P_{vi} is the i-th unit's transfer function from control to the output voltage, P_{ii} is the i-th unit's transfer function from control to the unit's current and Z_{outi}. is the output impedance of i-th unit.

In the form of transfer functions matrix, model of the complete power stage of parallel operating converters is given by:

$$\boldsymbol{y} = \begin{bmatrix} v_{out} \\ i_{L1} \\ i_{L2} \\ \vdots \\ i_{Ln} \end{bmatrix} = \begin{bmatrix} P'_{v1} & P'_{v2} & P'_{v3} & \ldots & P'_{vn} \\ P_{i1} & 0 & 0 & \ldots & 0 \\ 0 & P_{i2} & 0 & \ldots & 0 \\ \vdots & \vdots & \vdots & \ddots & \vdots \\ 0 & 0 & 0 & \ldots & P_{in} \end{bmatrix} = \boldsymbol{P}(s)\boldsymbol{u} \tag{12}$$

Since the output vector $\boldsymbol{y}$ is of dimension n+1 and there are only n independent input switch control signals, the transfer function matrix $\boldsymbol{P}$ is not square. One way to make it square, in order to obtain a closed-loop control, is to redefine the outputs

to represent the output voltage and the current distribution between the units [23]:

$$\boldsymbol{y} = [v_{out} \quad \Delta i_{L1} \quad \Delta i_{L2} \quad \dots \quad \Delta i_{Ln-1}]^T, \quad \Delta i_{Li} = i_{Li} - \sum_{j=1}^{n} \alpha_{ij} i_{Lj} \tag{13}$$

The transformation matrix

$$\boldsymbol{S} = \begin{bmatrix} 1 & 0 & 0 & 0 & \dots & 0 \\ 0 & -1 & 1 & 0 & \dots & 0 \\ 0 & -1 & 0 & 1 & \dots & 0 \\ \vdots & \vdots & \vdots & \vdots & \ddots & 0 \\ 0 & -1 & 0 & 0 & 0 & 1 \end{bmatrix} \tag{14}$$

introduces the current difference between the i-th unit and the reference (master) unit 0, making the redefined outputs of the squared plant $\boldsymbol{P}' = \boldsymbol{SP}$ fit into the *master-slave* (M-S) control configuration.

Multiplicative input uncertainty of the robust modeling is presented by the matrix expression:

$$\tilde{\boldsymbol{P}}(s) = \boldsymbol{SP}(s)(\boldsymbol{I} + \boldsymbol{L}_{MI}(s)\boldsymbol{\Delta}(s)) \tag{15}$$

where $\tilde{\boldsymbol{P}}(s)$ is the perturbed plant, $\boldsymbol{I}$ is the unity matrix, $\boldsymbol{\Delta}(s)$ is an unknown but unity-normed diagonal transfer function matrix that represents multiplicative uncertainty of the modeling and $\boldsymbol{L}_{MI}(s)$ is the diagonal multiplicative input uncertainty bound matrix:

$$\boldsymbol{L}_{MI}(s) = \operatorname{diag}(l^*_{MI1}(s), l^*_{MI2}(s), \dots, l^*_{MIn}(s)) \tag{16}$$

Transfer function $l^*_{MIi}(s)$ is the uncertainty bound for i-th channel of the control. Uncertainty associated matrices are diagonal because parametric uncertainty of every consisting unit is not dependent on the uncertainty of the others.

As for the single unit, bound of the multiplicative input channel uncertainties for the multivariable model should be developed to asymptotically describe the *parametric uncertainty* of the linear part of the circuitry: on low frequencies they should have the value of the maximal relative error of the model DC gain, then to rise with 20 dB per decade slope, reach 0 dB level before the half of the switching frequency and remain on the constant level in high frequencies.

If the output impedance is the same for all consisting units and it is negligible comparing to the load resistance, eq. (10) simplifies to:

$$v_{out}(s) \approx \frac{1}{\dfrac{n}{Z_{out}(s)}} \sum_{i=1}^{n} \frac{P_{vi}(s)}{Z_{out}(s)} d_i(s) = \frac{1}{n} \sum_{i=1}^{n} P_{vi}(s) d_i(s), \tag{17}$$

holding for most of the current-sharing applications having the same topology converters with the same parameters. Channel uncertainty is therefore the n-th part of n transfer functions uncertainties i.e.

$$l^*_{MIi}(s) = l_{MI}(s), \quad i = 1,2,\ldots n \tag{18}$$

where $l_{MI}(s)$ is the single unit deterministic (parametric) uncertainty bound, discussed previously in the power-stage uncertainty modeling. This is an important result because multivariable uncertainty bound can be constructed directly from the single unit uncertainty, which is much easier to obtain.

4 Framework for Robust Synthesis in the Closed Loop

The block diagram of control structure is presented in Fig. 9, where $\boldsymbol{r}$ denotes reference signals, $\boldsymbol{e} = \boldsymbol{r} - \boldsymbol{y}$ is error in reference tracking, $\boldsymbol{e}^{\prime}$ is the performance weighted error, $\boldsymbol{d}$ - plant input disturbance signal, and $\boldsymbol{K}$ is the closed-loop controller to be designed.

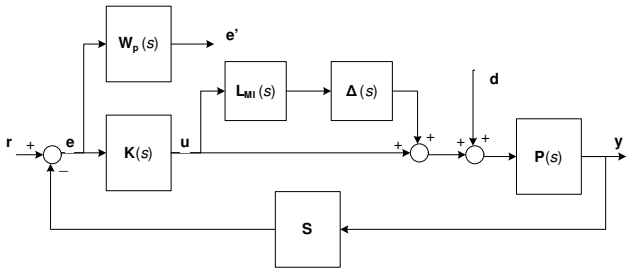

Fig. 9. Block diagram of control setup.

For the single unit design, setup is simplified for $\boldsymbol{L}_{MI}(s) = l_{MI}(s)$ and $\boldsymbol{S} = \boldsymbol{1}$. With the choice of the performance weighting function $\boldsymbol{W}_p(s)$, dependent on the specific control design, multivariable setup depicted in Fig. 9 is fully defined and ready for any robust control design procedure.

The objective that represents performance of the nominal closed-loop system is defined by the upper singular value

$$NP = \|np(\omega)\|_\infty = \|\boldsymbol{W}_p\boldsymbol{S}\|_\infty = \sup_\omega \overline{\sigma}(\boldsymbol{W}_p\boldsymbol{S}) < 1 \tag{19}$$

where NP is a measure of the nominal performance and $\boldsymbol{S}$ is sensitivity function.

The robust control theory adopts measures of robust stability (RS) and robust performance (RP) as a suitable objectives that define performance of the closed

loop system in the presence of structured uncertainty:

$$RS = \|rs(\omega)\|_\infty = \|\boldsymbol{L}_{MI}(\omega)\boldsymbol{T}(\omega)\|_\mu = \sup_\omega \mu_\Delta(\boldsymbol{L}_{MI}(\omega)\boldsymbol{T}(\omega)) < 1 \qquad (20)$$

$$RP = \|rp(\omega)\|_\infty = \left| \begin{matrix} \boldsymbol{W}_p(\omega)\boldsymbol{S}(\omega) & 0 \\ 0 & \boldsymbol{L}_{MI}(\omega)\boldsymbol{T}(\omega) \end{matrix} \right|_\mu = \sup_\omega \left(\begin{bmatrix} \boldsymbol{W}_p\boldsymbol{S} & 0 \\ 0 & \boldsymbol{L}_{MI}\boldsymbol{T} \end{bmatrix} \right) < 1, \qquad (21)$$

where $\boldsymbol{T}(\omega)$ is the complementary sensitivity function. The operator μ_Δ is structured singular value (μ-norm) computed according to the diagonal structure of uncertainty matrix $\boldsymbol{\Delta} = \text{diag}(\Delta_p, \Delta_q)$.

Objectives (19), (20) and (21) ensure that the closed-loop system cannot be destabilized by unknown but unity bounded matrix $\boldsymbol{\Delta}_p$, $\boldsymbol{\Delta}_q$ and $\boldsymbol{\Delta}$, respectively. The concept of the *NP*, *RS* and *RP* can be understood as the demand that the loop gain of the corresponding closed-loop system should be less than 1 at any frequency.

The convenient objective for synthesis of robust controller $\boldsymbol{K}$ using μ-norm is

$$\min_k RP, \text{ with constraint} RS < 1. \qquad (22)$$

Optimization can be done with respect to either reference signal $\boldsymbol{r}$, ensuring optimal reference tracking, or input disturbance signal $\boldsymbol{d}$ - ensuring optimal input disturbance rejection.

Once when control design is obtained, zero-pole cancellation can be applied and dynamics higher then the half of the switching frequency should be neglected.

5 Design Examples

5.1 Random control of the single unit buck converter

Prototype buck DC/DC converter parameters are: $f_{sw} = 50\text{kHz}$, $V_{IN} = 10\text{V}$, $I_G = 10\text{A}$, $V_{OUT} = 5\text{V}$, $R = 0.5\Omega, L = 50\mu\text{H}$, $R_L \approx 46\text{m}\Omega$, C = $4700\mu\text{F}$, $R_C \approx 24\text{m}\Omega$.

Converter nominal model is given by the transfer function from the control variable d to the output voltage v_{out}. According to Table 1, for the buck converter of interest that is:

$$P_v(s) = \frac{9.16(\frac{s}{8865} + 1)}{\frac{s^2}{2106^2} + \frac{s}{2487} + 1} \qquad (23)$$

Following guidelines given above, uncertainty bound DC value of 0.5 gives room for parameter variations that change transfer function in bounds of $\pm 50\%$.

Nominal model of the converter, along with the measured frequency response of the prototype (curve interpolated through experimentally obtained data) is presented in Fig. 10. Difference between the model and experimental data become significant

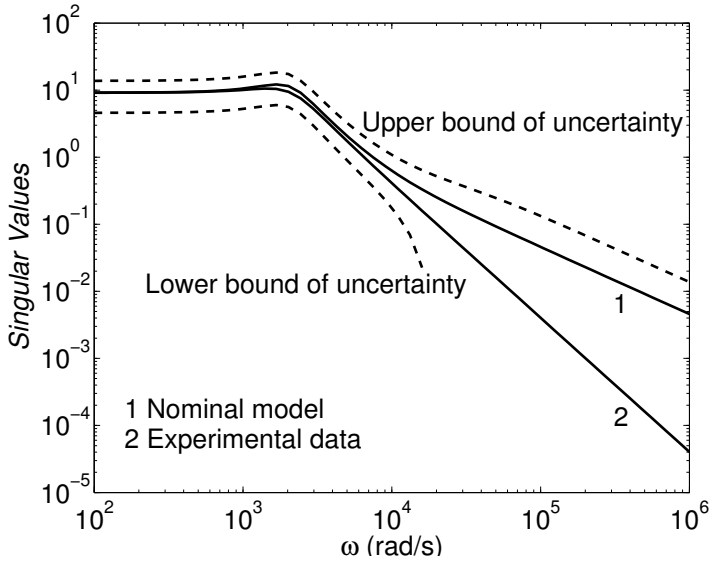

Fig. 10. Uncertainty bounds of the prototype buck DC/DC converter.

at frequencies above 10^4 rad/s, demanding increase of modeling uncertainty bound by positioning transfer zero before 10^4 rad/s. Control, to be designed later on, will have typical bandwidth of 1 - 2 kHz (3.14 - 6.28 krad/s), so $T_{WC}(s)$ should provide the bandwidth of at least 6.28 krad/s. Transfer zero is placed on frequency $\omega_0 = 9$ krad/s, towards higher bound, providing maximum bandwidth possibilities for control and uncertainty raise early enough to cover disagreements between the model and prototype frequency response. Pole of the $l_{MI}(s)$ is consequently placed on frequency $4 \cdot \omega_0$. Proposed deterministic modeling uncertainty bounds (also depicted in Fig. 10) are given with:

$$l_{DET}(s) = 0.5 \frac{\frac{s}{\omega_o} + 1}{\frac{s}{4\omega_o} + 1}, \quad \omega_0 = 9000\text{rad/s} \tag{24}$$

Uniform distribution is selected for randomization of appropriate variables and un-

certainty bound of the modeling is finally:

$$l_{MI}(s) = (0.5+R)\frac{\dfrac{s}{\omega_0}+1}{\dfrac{s}{4\omega_0}+1}, \quad \omega = 9000\text{rad/s} \tag{25}$$

where R is maximal excursion of the control variable due to randomness.

Robust performance specification W_p is selected to ensure zero steady-state in reference tracking, +20 dB per decade growth of sensitivity operator in the low frequency range, regulation bandwidth of 2000 rad/s and worst case robust sensitivity peak value of 2. Appropriate transfer function for such description is:

$$W_p(s) = \frac{1}{2}\frac{\dfrac{s}{2000}+1}{s} \tag{26}$$

Seven controllers are designed, resulting μ-optimal parameter tuning of fixed structure controllers or synthesized full order controllers [13]-[16]:

1. *muIMCrt* - IMC μ-optimal for reference tracking, fixed structure, one tunable parameter ω_1 depicted in Fig. 11 a) for increasing projected random level R.
2. *muIMCdr* - IMC μ-optimal for input disturbance rejection, fixed structure, one tunable parameter ω_1 depicted in Fig. 11 b).

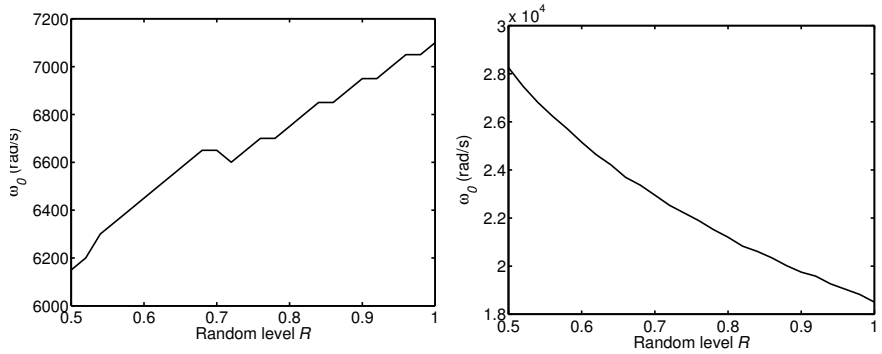

Fig. 11. Parameter ω_1 of *muIMC* controllers; (a) *muIMCrt*, (b) *muIMCdr*.

3. *lsdp* - full order H_∞ Loop Shaping Controller [16] is not subject of change with increase of R because its design is based on nominal performance, and robust stabilization is in the closed form of Glover-Doyle compensator, again not dependent on R. Design parameters for *lsdp* are:

$$K_p = 4000, \quad \omega_p = 3000\text{rad/s}; \quad \varepsilon_{max} = 0.53 \tag{27}$$

$$K_{LSDP} = \frac{2.089(s+3000)(s^2+5157s+8.972\times10^6)}{s(s+3030)(s+7354)} \tag{28}$$

4. *muopt3rt* - full order μ-suboptimal for reference tracking, second D-K iteration with 3^{rd} order D interpolation. For $R=0$ it is deterministic controller:

$$\mu_{3rt}(s) = \frac{3.02(s+887.7)(s+3.6\times10^4)(s+6.42\times10^4)(s^2+2578s+2.66\times10^6)}{s(s+699.8)(s+8906)(s+4.75\times10^4)(s+8.33\times10^4)} \tag{29}$$

When R is increasing, controller transfer function zeros and poles do change place, but dominant behavior of the control is due to the velocity constant change, presented in Fig. 12 a).

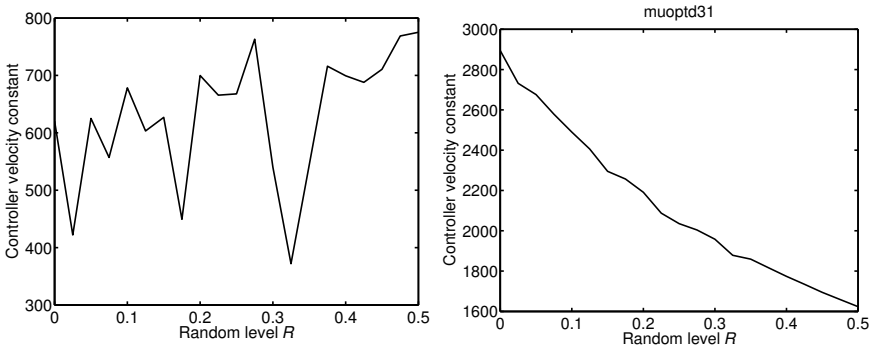

(a) (b)

Fig. 12. Velocity constant of *uopt*3 controllers: (a) *mu opt rt*, (b) *mu opt dr*.

5. *muopt3dr* - full order μ-suboptimal for input disturbance rejection, second $D-K$ iteration with 3^{rd} order D interpolation. As for the *muopt*3*rt*, with $R=0$ controller is deterministic:

$$\mu_{3dr}(s) = \frac{7.23(s+3.441\times10^4)(s^2+4160s+7.174\times10^6)}{s(s+8865)(s+6.721\times10^4)} \tag{30}$$

Velocity constant of the *muopt3dr*, with R increasing, is depicted in Fig. 12 b).

6. *muPIrt* - PI μ-optimal for reference tracking, fixed structure, two tunable parameters: $K_p = 10^4$ and ω_n changing in the manner presented in Fig. 13 a).
7. *muPIdr* - PI μ-optimal for input disturbance rejection, fixed structure, two tunable parameters: $K_p = 10^4$ and ω_n changing as depicted in Fig. 13 b).

All control solutions' *RP*, *RS* and *NP* measures for different random levels R are given in fig. 14 a), b) and c), consequently.

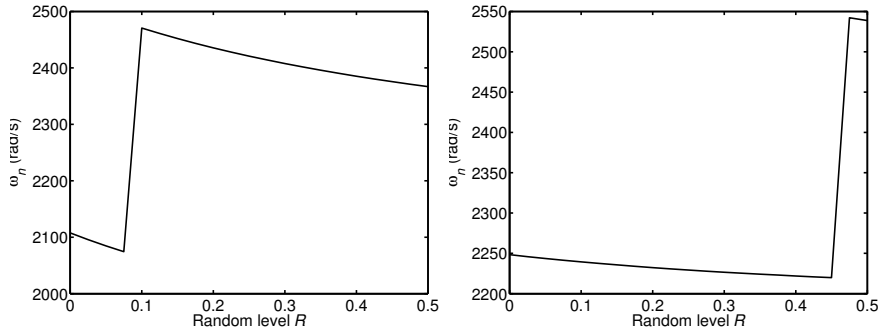

Fig. 13. Parameter ω_n of *mu PI* controllers: (a) *mu PI rt*, (b) *nu PI dr*.

Both PI controllers don't satisfy robust stability condition $RS < 1$ at any randomness level, so they are not considered perspective for further discussion. *RP* measure is higher for *mu IMC dr* and $lsdp$ comparing to the rest of the controllers due to higher values of *RS* in the whole range of applied R, indicating worse performance of *mu IMC dr* and $lsdp$ solutions under large scale perturbations of the plant.

All controllers have *RS* at level of 1 approximately up to $R = 0.2$, but only *mu IMC rt* and *mu opt3 rt* have the possibility to go further in increase of R. Random level $R = 0.2$ will be taken, therefore, as the fair reference point for further controller analysis. In order to verify control design and spectral formulas, simulation is performed on nonlinear $Matlab/Simulink$ model of the converter. Dynamic behavior of closed loop systems with AFIX modulation and $R = 0.2$ is presented in Fig. 15.

Optimal reference tracking is achieved with $lsdp$. Disturbance rejection is the best with *mu* $opt3$ dr, considering peak response on disturbance, but the quickest elimination is with $lsdp$. Both *rt* controllers: *mu IMC rt* and *mu opt3 rt* are having unsatisfactory disturbance elimination, essential characteristic for DC/DC converter control, so they are not acceptable solutions in random switching control.

5.2 Deterministic control of the three paralleled buck units

Parameters of the general power supply setup is: $V_{IN} = 10$V, $V_{OUT} = 5$V, $I_{OUT} = 30$A. Each of the three buck DC/DC unit has the parameters: $f_{sw} = 50$kHz, $L = 50\mu$H, $R_L \approx 46$mΩ, $C = 4700\mu$F, $R_C \approx 24$mΩ.

Maximum allowed uncertainty of the modeling is proposed in the same way as

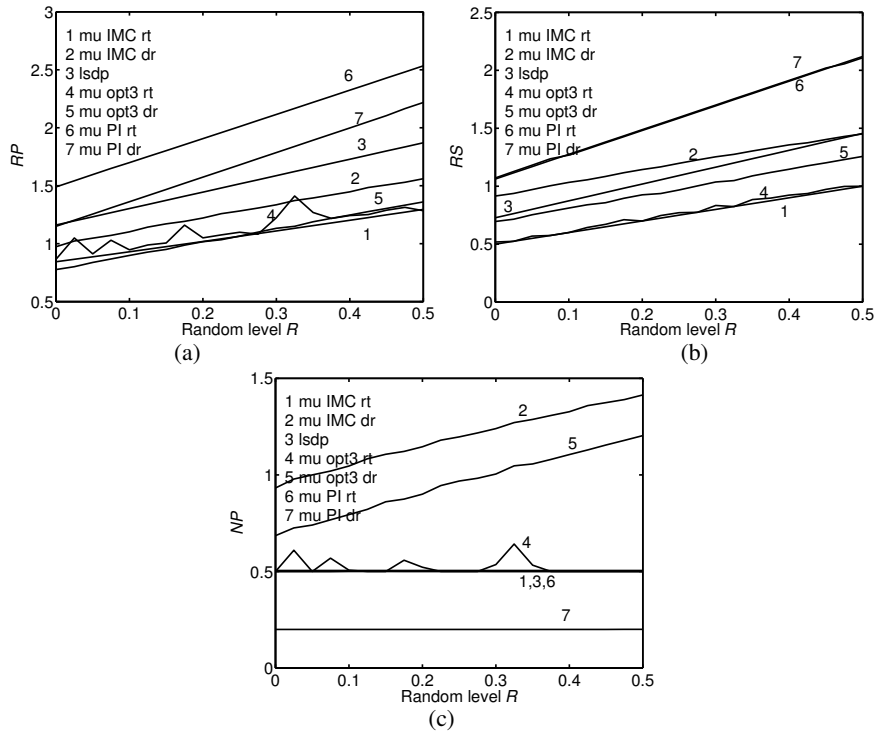

Fig. 14. Performance and stability measures for different random levels R: (a) robust performance RP, (b) robust stability RS, (c) nominal performance NP.

for the single unit case:

$$l^*_{MI}(s) = 0.5\frac{\frac{s}{\omega_0}+1}{\frac{s}{4\omega_0}+1}, \qquad \omega_0 = 9000\text{rad/s} \tag{31}$$

so the control in the closed loop will be tested for robustness according to proposed measure.

Nominal (M-S squared) model of the three parallel operating converters is given by:

$$\boldsymbol{P}'(s) = \frac{2.97}{\frac{s^2}{4.4310^6}+\frac{s}{1783}+1}\begin{bmatrix} 6.15(\frac{s}{8865}+1) & 6.15(\frac{s}{8865}+1) & 6.15(\frac{s}{8865}+1) \\ -(\frac{s}{405}+1) & \frac{s}{405}+1 & 0 \\ -(\frac{s}{405}+1) & 0 & \frac{s}{405}+1 \end{bmatrix} \tag{32}$$

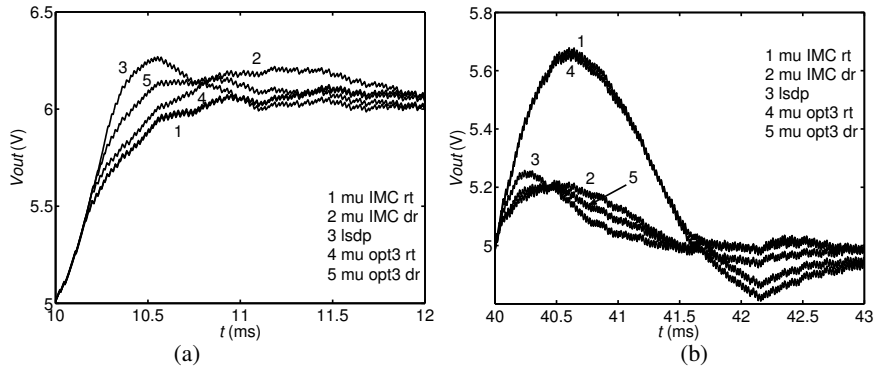

Fig. 15. Buck DC/DC converter nonlinear model control with AFIX and $R = 0.2$: (a) output voltage response to voltage reference step, (b) output voltage response to input disturbance step ($d = 0.4$).

Robust performance specification $\boldsymbol{W}_p$ is selected to ensure zero steady-state in reference tracking, +20dB per decade growth of sensitivity operator in the low frequency range, regulation bandwidth of 2000 rad/s and worst case robust sensitivity peak value of 1.4. Appropriate transfer function for such description is:

$$\boldsymbol{W}_p(s) = \frac{1}{1.4}\frac{\frac{s}{2000}+1}{s}\boldsymbol{I}_3 \tag{33}$$

Three robust controllers are obtained: H_∞ reference tracking controller ($H_\infty rt$) [14, 15], μ-optimal IMC reference tracking (*muIMCrt*) [13, 14] and H_∞ loop-shaping controller ($lsdp$) [14, 16]. After zero-pole cancellation and diagonalization, voltage-loop and current loop controllers for master-slave control are obtained and enlisted in Table 2. Final robust controllers are of simple PI/PID type.

Projected uncertainty bound along with the permitted uncertainty achieved with originally designed and diagonalized controllers are presented in Fig. 16.

It can be observed that the uncertainty level provided by the $H_\infty rt$ is not preserved after diagonalization and it is far bellow satisfactory. Controller *muIMCrt* has the best robustness properties, while $lsdp$ control in the closed loop violates the proposed bound (31). However, this happens in the frequency region where more than 100% uncertainty is demanded, so it doesn't influence the robustness of the designed $lsdp$ solution.

In order to verify control design performance and robustness in the time-domain, simulation is performed on nonlinear *Simulink* model of the converters with PWM and M-S control scheme fully implemented. The parameters of the second slave converter are changed to $L' = 0.75L$, $C' = 0.75C$, $V'_{in} = 0.9V_{in}$. Load current consumption change of 33% is given (from 30A to 40A) and dynamic behavior of the perturbed slave current is presented in Fig. 17 a).

Table 2. Robust controllers for three buck setup

Robust Design	Voltage and current-loop controllers
lsdp	$K_v(s) = \dfrac{2.56(s^2+7328s+1.43\times10^6)}{s(s+8046)}$ $K_i(s) = \dfrac{0.5(s+300)}{s}$
$H_\infty rt$	$K_v(s) = \dfrac{692.4\left(\dfrac{s^2}{5.78\times10^6}+\dfrac{s}{3730}+1\right)}{s\left(\dfrac{s}{6.2\times10^4}+1\right)\left(\dfrac{s^2}{1.02\times10^8}+\dfrac{s}{1.91\times10^4}+1\right)}$ $K_i(s) = \dfrac{0.33(s+2711)}{s}$
muIMCrt	$K_v(s) = \dfrac{0.31(s^2+1903s+4.5\times10^6)}{s(s+8865)}$ $K_i(s) = \dfrac{0.0047(s^2+1783s+4.4\times10^6}{s(s+405)}$

The dynamic response quality is mainly kept with all the controllers after diagonalization. The best response is with *lsdp*, while $H_\infty rt$ and *IMCrt* exhibit current overshoots and are of lower bandwidth.

As *lsdp* has shown the best properties in the closed loop, it was implemented

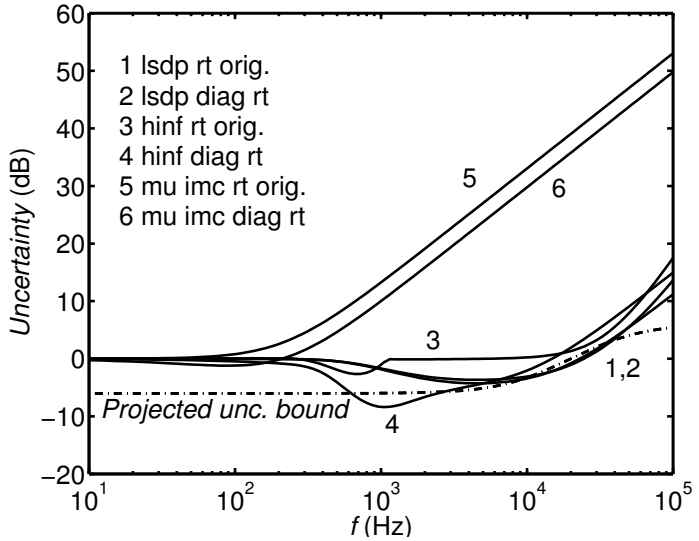

Fig. 16. Projected and achieved uncertainty for designed controllers (three buck setup).

in analog technique and tested in the same setup within the *pSpice* circuit-oriented environment. Dynamic response of the perturbed unit's current with the *pSpice* model is presented in Fig. 17 b).

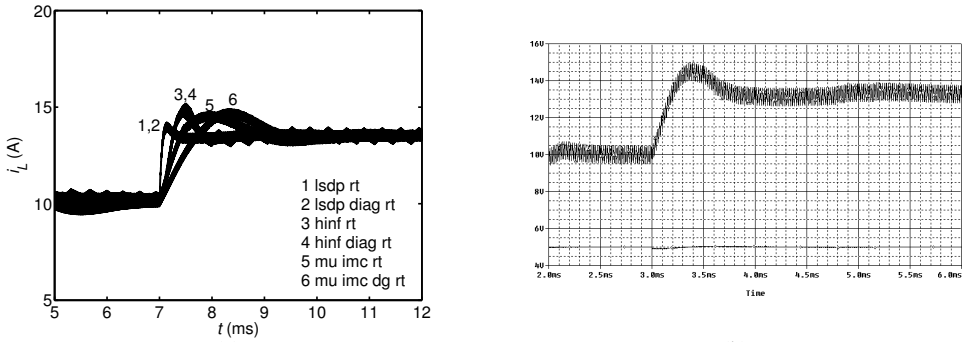

(a) (b)

Fig. 17. Current dynamics of the perturbed plant on load consumption step-change ($\Delta I_{OUT} = 33\%$): (a) all controllers within the nonlinear *Simulink* model, (b) *lsdp* within *pSpice* model.

The *pSpice* simulation validates the results of *ldsp* linear design both in performance and robustness aspect.

6 Conclusion

Complex robust control theory was used to obtain simple controllers for both single and current-sharing DC/DC converters. Methodology for construction of the converter's power stage nominal model is proposed and uncertainty bounds of the modeling are considered for parametric uncertainty, nonlinear effects in control, CMC switching effects and random control. Robust model is developed also for the current-sharing configuration of the converters. Unified approach to the frequency domain control synthesis is proposed, several robust controllers are designed and verified in *Matlab*/*Simulink* and in *pSpice* on random single buck unit and deterministic three buck unit setup.

Main drawbacks of linear robust theory are circumvented: linear time invariant model of wide range single and paralleled converters is posed for both deterministic and random control, frequency domain weighting functions (as tuning parameters of the control design) are simple and tightly attached to design requirement and high order controllers are simplified to the level of standard PI/PID controllers, making them easy to implement in both analog and digital control systems.

References

[1] N. Mohan *et al.*, *Power Electronics*. NY-USA: John Willey, 1995.

[2] D. M. Mitchell, *DC/DC Switching Regulator Analysis*. NY-USA: McGraw-Hill, 1988.

[3] R. B. Ridley, "A new continuous-time model for current-mode control," *IEEE Trans. On Power Electronics*, vol. 6, no. 2, pp. 271–280, 1991.

[4] L. R. Lewis, B. H. Cho, F. C. Lee, and B. A. Carpenter, "Modeling and analysis of distributed power systems," in *Proc. IEEE PESC'89*, 1989, pp. 152–159.

[5] B. Choi, B. H. Cho, R. B. Ridley, and F. C. Lee, "Control strategy for multi-module parallel converter systems," in *Proc. Conf. Rec. PESC'90*, 1990, pp. 225–234.

[6] K. Siri, C. Lee, and T. F. Wu, "Current distribution for parallel connected converters: Part i," *IEEE Trans. Aerosp. Electron. Syst.*, vol. 28, pp. 829–840, July 1992.

[7] Y. Panov, J. Rajagopalan, and F. C. Lee, "Analysis and control design of n paralleled dc-dc converters with master-slave current sharing control," in *Proc. Applied Power Electronics Conference '97*, 1997, pp. 436–442.

[8] V. J. Thottuvelil and G. C. Verghese, "Analysis and control design of paralleled DC/DC converters with current sharing," *IEEE Trans. Power Electron.*, vol. 13, pp. 635–644, July 1998.

[9] B. Choi, "Comparative study on paralleling schemes of converter modules for distributed power applications," *IEEE Trans. Ind. Electron.*, vol. 45, pp. 194–199, Apr. 1998.

[10] P. Li and B. Lehman, "A design method for paralleling current mode controlled dc-dc converters," *IEEE Trans. Power Electron.*, vol. 19, pp. 748–756, May 2004.

[11] M. López, L. G. de Vicuña, M. Castilla, P. Gayà, and O. López, "Current distribution control design for paralleled DC/DC converters using sliding-mode control," *IEEE Trans. Ind. Electron.*, vol. 51, pp. 419–428, 2004.

[12] B. Tomescu and H. F. VanLandingham, "Improved large-signal performance of paralleled dc-dc converters current sharing using fuzzy logic control," *IEEE Trans. Power Electron.*, vol. 14, pp. 573–577, May 1999.

[13] M. Morari and E. Zafiriou, *Robust Process Control*. NY-USA: Prentice Hall, 1989.

[14] S. Skogestad and I. Postlethwaite, *Multivariable Feedback Control*. England: John Willey & Sons, 1996.

[15] K. Zhou *et al.*, *Robust and Optimal Control*. NJ-USA: Prentice Hall, 1996.

[16] D. C. McFarlane and K. Glover, *Robust Controller Design Using Normalized Coprime Factor Plant Description*. Germany: Springer-Verlag, 1990.

[17] S. Buso, "Design of a robust voltage controller for a buck-boost converter using μ synthesis," *IEEE Trans. Contr. Syst. Tech.*, vol. 7, pp. 222–229, Mar. 1999.

[18] T. B. Petrović and A. Ž. Rakić, "Modelling and robust controllers for deterministic switching DC/DC converters," in *Proc. Yugoslav Power Electronics Conference*, 2001, pp. 374–382.

[19] ——, "Linear robust approach to DC/DC converter modeling: Part i - deterministic switching," *Electrical Engineering*, vol. 86, pp. 267–274, Sept. 2004.

[20] ——, "Linear robust control of DC/DC converters: Part i - deterministic switching," *Electrical Engineering*, vol. 87, pp. 57–68, Feb. 2005.

[21] A. Ž. Rakić and T. B. Petrović, "Linear robust approach to DC/DC converter modeling: Part ii - random switching," *Electrical Engineering*, vol. 86, pp. 275–284, Sept. 2004.

[22] ——, "Linear robust control of DC/DC converters: Part ii - random switching," *Electrical Engineering*, vol. 87, pp. 69–96, Feb. 2005.

[23] D. S. Garabandić and T. B. Petrović, "Modeling parallel operating pwm DC/DC power supplies," *IEEE Trans. Ind. Electron.*, vol. 42, pp. 545–551, Oct. 1995.

[24] A. Ž. Rakić, T. B. Petrović, and D. M. Dujković, "Linear robust approach to modeling of parallel operating DC/DC converters," in *Proc. INDEL Conference*, Nov. 2004, pp. 54–59.

[25] R. Tymerski, "Worst-case stability analysis of switching regulators using the structured singular value," *IEEE Trans. Power Electron.*, vol. 11, pp. 723–730, Sept. 1996.

[26] T. B. Petrović and S. M. Vasilić, "Robust decentralized controllers with disturbance rejection for parallel operating DC/DC converters," *Control and Computers*, vol. 25, no. 3, pp. 80–87, 1997.

[27] S. M. Vasilć and T. B. Petrovć, "Design of advanced robustdecentralized control of parallel DC/DC converters," *Electrical Engineering*, no. 1, pp. 27–34, 1998.

[28] T. B. Petrović and A. Ž. Rakić, "The loop shaping design procedure for parallel operating DC/DC converters," *Electrical Engineering*, vol. 82, no. 3-4, pp. 217–224, 2000.